ELSEVIER

Journal of Power Sources 101 (2001) 238–247

JOURNAL OF POWER SOURCES

www.elsevier.com/locate/jpowsour

An accelerated calendar and cycle life study of Li-ion cells

I. Bloom[a,*], B.W. Cole[a], J.J. Sohn[a], S.A. Jones[a], E.G. Polzin[a], V.S. Battaglia[a], G.L. Henriksen[a], C. Motloch[b], R. Richardson[b], T. Unkelhaeuser[c], D. Ingersoll[c], H.L. Case[c]

[a]*Electrochemical Technology Program, Argonne National Laboratory, 9700 South Cass Avenue, Argonne, IL 60439, USA*
[b]*Idaho National Engineering and Environmental Laboratory, Idaho Falls, ID 83415, USA*
[c]*Sandia National Laboratories, Albuquerque, NM 87185, USA*

Received 8 February 2001; accepted 15 February 2001

Abstract

The accelerated calendar and cycle life of lithium-ion cells was studied. Useful cell life was strongly affected by temperature, time, state-of-charge (SOC) and change in state-of-charge (ΔSOC). In calendar life experiments, useful cell life was strongly affected by temperature and time. Temperature accelerated cell performance degradation. The rates of area specific impedance (ASI) increase and power fade followed simple laws based on a power of time and Arrhenius kinetics. The data have been modeled using these two concepts and the calculated data agree well with the experimental values.

The calendar life ASI increase and power fade data follow $(\text{time})^{1/2}$ kinetics. This behavior may be due to solid electrolyte interface layer growth. From the cycle life experiments, the ASI increase data follow $(\text{time})^{1/2}$ kinetics also, but there is an apparent change in overall power fade mechanism when going from 3 to 6% ΔSOC. Here, the power of time drops to below 1/2, which indicates that the power fade mechanism is more complex than layer growth.

Keywords: Accelerated life study; Li-ion cells; Arrhenius kinetics; Parabolic (VE) kinetics

1. Introduction

Lithium-ion rechargeable batteries have attracted the interest of many research groups and industries. Typically, these batteries consist of lithiated-carbon intercalation anodes, a liquid electrolyte containing a lithium salt, and a lithium insertion cathode (usually Li_xNiO_2, Li_xCoO_2 or $Li_xMn_2O_4$). In its goal of developing an 80 mpg vehicle, the partnership for a new generation of vehicles (PNGV) is focusing its energy storage R&D efforts on high-power Li-ion batteries to meet its energy storage requirements for leveling the load on a prime power source and for capturing regenerative braking energy. The industrial developers have demonstrated that the Li-ion battery technology is capable of meeting the performance and cycle life requirements for this application, but these barriers to commercialization remain: calendar life, thermal abuse, and safety.

Three national laboratories collaborated in the characterization and testing of 18,650 cells, which utilize a generic Li-ion chemistry. The goal for this project was to develop an understanding of the effect of accelerated calendar life testing on the performance of Li-ion cells, especially on the resistance and power of the cells. By observing and modeling the changes in these parameters, we were able to project the calendar life at room temperature.

2. Experimental

2.1. Cells and cell testing

Sixty 0.9 Ah, 18,650 cells were fabricated to our specification for this study. The exact chemistry of these cells is summarized in Table 1.

The cathodes and anodes were cast as thin films on ca. 1 m aluminum and copper foils, respectively, to yield an effective active area of 678 cm^2. After assembly, the cells underwent a few formation cycles and a 21-day stand before shipment to the test labs. The ratings of the cells are given in Table 2. The constant-current/-voltage charging algorithm is charge at C/1 until the battery voltage equals 4.1 V and potentiostat at 4.1 V for a total of 2.5 h.

Each cell was characterized using standard battery test procedures given in the PNGV Battery Test Manual [1].

* Corresponding author. Tel.: +1-630-252-4516; fax: +1-630-252-4176.
E-mail address: bloom@cmt.anl.gov (I. Bloom).

0378-7753/01/$ – see front matter
PII: S0378-7753(01)00783-2

Table 1
Cell chemistry

Positive electrode	Negative electrode
8 wt.% PVDF binder	9 wt.% PVDF binder
4 wt.% SFG-6 graphite	16 wt.% SFG-6 graphite
4 wt.% carbon black	75 wt.% MCMB-6 graphite
84 wt.% $LiNi_{0.8}Co_{0.2}O_2$	
Electrolyte	Separator
1 M $LiPF_6$ in EC/DEC (1:1)	37 μm thick PE Celgard separator

Table 2
Cell ratings

Parameter	Value
Maximum voltage (V)	4.1 continuous; 4.3 pulse
Minimum voltage (V)	3.0
Maximum discharge current (A)	8.0 pulse; 2.0 continuous

Among the characterization tests used were the C/1 capacity and the hybrid pulse power capability test using the medium current level (HPPC-M) at 7.2 A.

For both calendar and cycle life, fixed voltages defined all the states-of-charge (SOC). These voltages were determined by performing a C/25 rate discharge at 25°C on a group of six cells. The values of 3.918, 3.747, and 3.600 V at 25°C represent 80, 60 and 40% SOC, respectively.

2.2. Calendar life

Accelerated calendar life testing consisted of exposing cells to the conditions given in the test matrix at the laboratories indicated in Table 3. Each entry in Table 3 represents a set of three cells exposed to a given set of conditions. Thus, a total of six cells were exposed to each of four temperatures (i.e. 40, 50, 60 and 70°C) and to each of two SOCs (60 and 80%). Three additional cells were exposed to each of the four temperatures listed at 40% SOC.

The fully-charged cells were discharged at the C/1 rate to a voltage representing the desired SOC (see above). After voltage equilibration for 2.5 h, the cells were heated to the target temperatures and the voltages were allowed to drift. The cells were then potentiostated at the new voltage for 4 weeks for the cells at 40, 50 and 60°C and 2 weeks for the cells at 70°C (thermal soak periods).

Additional information was gathered during the thermal soak periods. Because of different equipment at the three test labs, two types of calendar life tests were performed. The ANL measured the leakage current (group A), and SNL and INEEL conducted the special calendar test [2] (group B).

2.3. Cycle life

Accelerated cycle life testing consisted of exposing cells to the conditions given in the test matrix at the laboratories indicated in Table 4. These conditions exposed three cells to each of four temperatures (40, 50, 60 and 70°C), to each of two SOCs (60 and 80%), and to two ΔSOCs (3 and 6%). The ΔSOC is defined as the amount of nominal capacity of the cell discharged during a current pulse. The 3% ΔSOC life cycle profile is given in Fig. 1 and Table 5. It consisted of an 18 s discharge and 2 s regen (regen stands for ''regenerative breaking,'' which is a charge pulse) sequence followed by a 32 s bulk charge, which was followed by a taper charge. The 6% ΔSOC consisted of two consecutive discharge pulses followed by two consecutive regen pulses. Three additional cells were exposed to 60°C, 60% SOC, and 6% ΔSOC. The 6% ΔSOC profile consisted of two discharge-regen sequences in series followed by a twice as long bulk charge.

Table 3
Test matrix for accelerated calendar life study[a]

SOC (%)	Temperature (°C)			
	40	50	60	70
40	ANL	ANL	ANL	ANL
60	ANL, INEEL	ANL, INEEL	ANL, INEEL	ANL, INEEL
80	INEEL, SNL	INEEL, SNL	INEEL, SNL	INEEL, SNL

[a] ANL: Argonne National Laboratory; INEEL: Idaho National Engineering and Environmental Laboratory; SNL: Sandia National Laboratories.

Table 4
Test matrix for accelerated cycle life study

SOC (%)	ΔSOC (%)	Temperature (°C)			
		40	50	60	70
80	3	SNL	SNL	INEEL	SNL
	6	SNL	SNL	INEEL	SNL
60	3	INEEL	INEEL	INEEL	INEEL
	6	INEEL	INEEL	INEEL, ANL	INEEL

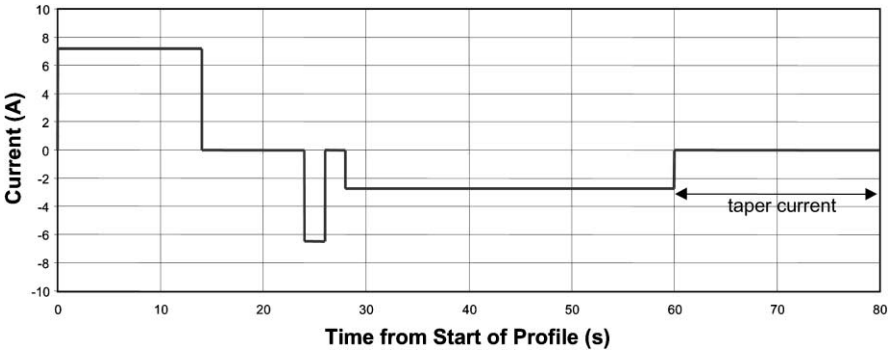

Fig. 1. Cycle life pulse profile for 3% ΔSOC.

2.4. Reference performance tests

Changes in cell performance were measured by using reference performance tests (RPTs). The RPTs were performed after each thermal soak period; the cells were cooled to 25°C. The RPTs consisted of a C/1 discharge capacity (static capacity) test and the HPPC-M test. The HPPC-M test consisted of charging the cell to 100% SOC and performing a C/1 discharge to remove 10% of the capacity of the cell followed by a 1 h rest. The HPPC-M profile [3] was then performed at 90% SOC. From then on, the process was repeated, except that the 10% capacity removed included the capacity used in the HPPC-M profile. Cells were taken off test at either a fixed time (8–12 weeks) or when they could not complete the sixth HPPC-M pulse.

2.5. Analysis and modeling of test data

The raw RPT HPPC-M data were reduced to produce discharge and regen area-specific impedance (ASI) and power versus SOC curves. The ASI values were determined from $\Delta V/\Delta I$ calculations for each iteration of the test profile according to the following equations and Fig. 2.

$$\text{Discharge resistance} = \frac{\Delta V}{\Delta I} = \frac{V_{t0} - V_{t1}}{I_{t0} - I_{t1}}$$

$$\text{Regen resistance} = \frac{V_{t3} - V_{t4}}{I_{t3} - I_{t4}}$$

$$\text{Discharge ASI} = 678\,\text{cm}^2 \times \text{discharge resistance}$$

$$\text{Regen ASI} = 678\,\text{cm}^2 \times \text{regen resistance}$$

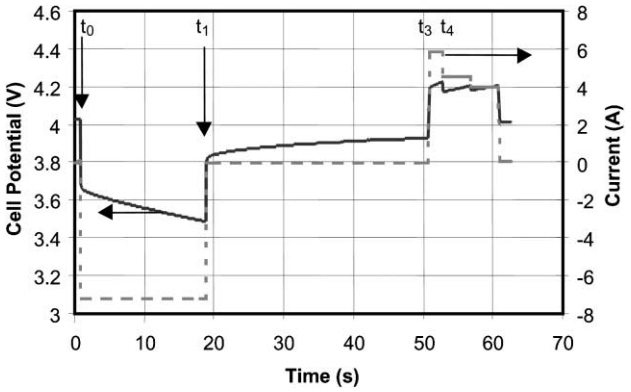

Fig. 2. Cell potential and current vs. time for an HPPC-M pulse profile. Voltage is the solid line, and current is the dashed line.

Pulse power capability is calculated from the resistance values and an interpolated open circuit voltage (OCV). The OCV value is taken from the data points immediately before the profile for each discharge step. The equations used to calculate power are given below

$$\text{Discharge pulse power} = V_{\min}\frac{\text{OCV} - V_{\min}}{\text{discharge resistance}}$$

$$\text{Regen pulse power} = V_{\max}\frac{V_{\max} - \text{OCV}}{\text{regen resistance}}$$

where $V_{\max} = 4.1$ V and $V_{\min} = 3.075$ V.

The derived HPPC-M resistance and power values from the three test labs were pooled, averaged, and analyzed for trends. Arbitrarily, the 60% SOC data (cell voltage = 3.75 V)

Table 5
Life cycle 3% ΔSOC pulse profile

Step time (s)	Cumulative time (s)	Current (A)	Charge (A s)	Cumulative charge (A s)
14	14	7.20	100.80	100.80
10	24	0.00	0.00	100.80
2	26	−6.48	−12.96	87.84
2	28	0.00	0.00	87.84
32	60	−2.745	−87.84	0.00
20	80	–[a]	–	–

[a] Adjust CV as necessary, starting with OCV–SOC.

from the HPPC-M tests were used. Where necessary, the value at 60% SOC was approximated by linear interpolation using the FORECAST function in Microsoft EXCEL. The data from cells that vented or leaked during the test were excluded from the analyses.

For the data from ANL and SNL, we looked for agreement of the percent change (within 1–2%) in the performance parameter at least between two out of the three cells. The data from INEEL was found to have strong cell-lot dependence and this dependence was used to select cells for further analyses and modeling.

The data were fit by the general equation

$$Q = A \exp\left(\frac{-E_a}{RT}\right) t^z$$

where Q is the ASI or power, A the pre-exponential factor, E_a the activation energy in J, R the gas constant, T the absolute temperature, t the time, and z the exponent of time. For simple diffusion control or layer growth, $z = 1/2$. This equation was linearized by taking the natural logarithm of both sides of the equation and using the EXCEL function LINEST to calculate ln A, E_a/R, and z. In addition, LINEST returned the standard error (S.E.) around each parameter and the regression coefficient, r^2.

3. Results and discussion

In general, the cells at higher temperatures failed before the ones at lower temperatures. For example, in both the calendar and cycle life tests, the 70°C cells failed after 2 weeks of testing. The ones at 60°C tended to fail after 4 weeks of testing. In addition to the temperature effect on life, cycling the cells and pulsing them during the calendar test tended to shorten their lives. Premature cell failure and cell leakage produced a sparse data matrix to analyze. The initial average values for the cell populations are given in Table 6. The average error around these values is 5–7%.

Table 6
Initial average values from cells in this study[a]

Test/group	ASI (Ω cm^2)	Power (W)
80% calendar life	49.73	43.83
60% calendar life/A	44.70	45.95
60% calendar life/B	50.08	30.12
40% calendar life	45.29	46.36
Cycle life (all SOCs and ΔSOCs)	49.09	36.11

[a] The values 80, 60 and 40% indicate the SOC; A indicates cells monitored for leakage current, B indicates cells subjected to one current pulse a day.

3.1. Calendar life

All data analyses focused on the changes in discharge ASI and power. Typical ASI versus SOC (as given by cell voltage) and power versus SOC curves are given in Figs. 3 and 4. The curves in these figures show expected trends: power decreases and ASI increases with time.

The parameters from all the fits are given in Table 7 for the three SOCs. The cells exposed to 70°C and 80% SOC failed very quickly. Very little ASI and power data were obtained under these conditions, and these cells were excluded from further analysis. Table 7 also contains the fitting results using the remaining temperature data at 40, 50, and 60°C. From the values of r^2, most of the fits are very good, and the data followed square-root of time (1D diffusion) and Arrhenius kinetics.

Plots containing ASI and power examples are given in Figs. 4–8, respectively, for the calendar tests. In these plots,

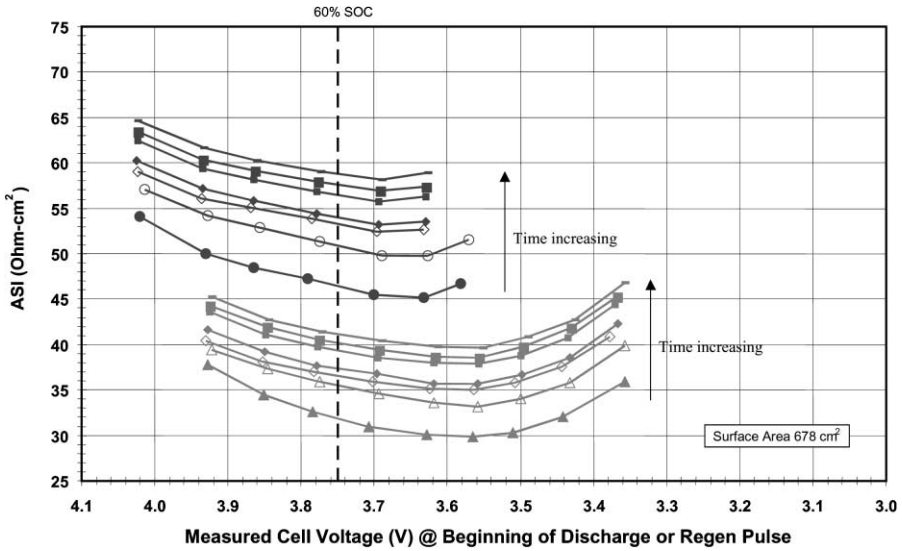

Fig. 3. Typical ASI vs. cell voltage plot derived from HPPC-M data. The lower set of curves is from the regen ASI and the upper is from discharge ASI. These curves represent seven sets of data spanning 28 weeks.

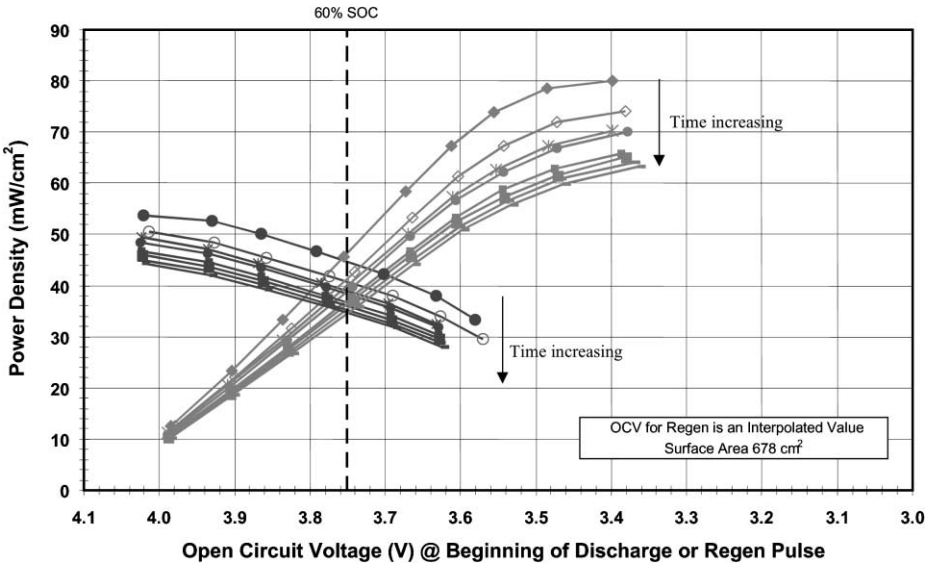

Fig. 4. Typical power density vs. cell voltage curves from HPPC-M data.

Table 7
The ASI change and power fade fitting parameters

SOC (%)/group		ASI increase				Power fade			
		z	E_a/R (K)	ln A	r^2	z	E_a/R (K)	ln A	r^2
40	Value	0.52	6827.30	23.1	0.98	0.44	6095.95	20.83	0.97
	S.E.	0.05	350.94	1.04		0.06	423.05	1.25	
60/A	Value	0.51	6810.67	23.49	0.99	0.46	5541.28	19.36	0.81
	S.E.	0.06	374.31	1.11		0.18	1086.14	3.21	
60/B	Value	0.51	4828.96	17.50	0.94	0.41	3820.41	14.31	0.93
	S.E.	0.16	759.73	2.18		0.13	636.16	1.83	
80	Value	0.61	2715.18	10.74	0.87	0.46	2262.09	9.47	0.83
	S.E.	0.14	719.42	2.18		0.15	750.39	2.27	

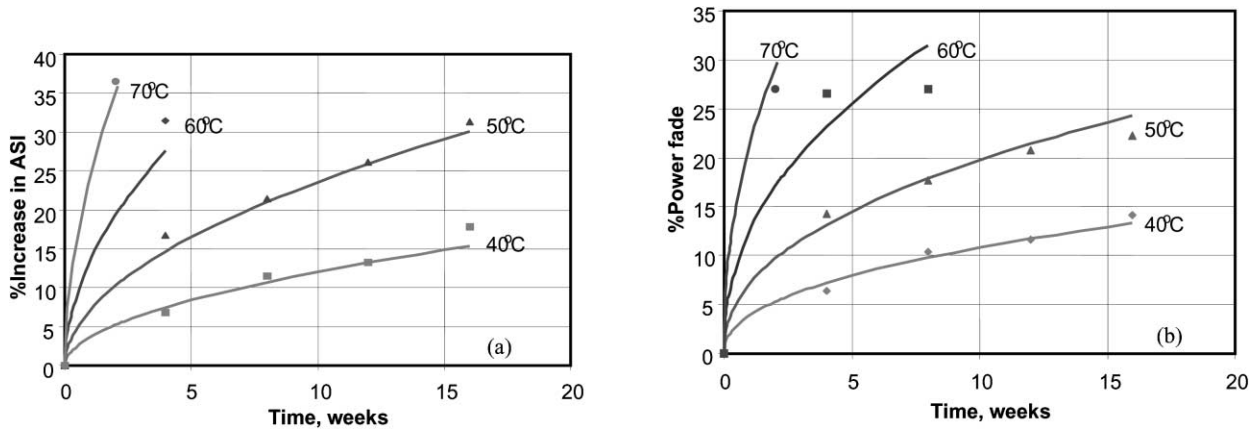

Fig. 5. (a) Increase in ASI and (b) power fade with time for calendar life at 40% SOC. Markers represent experimental values.

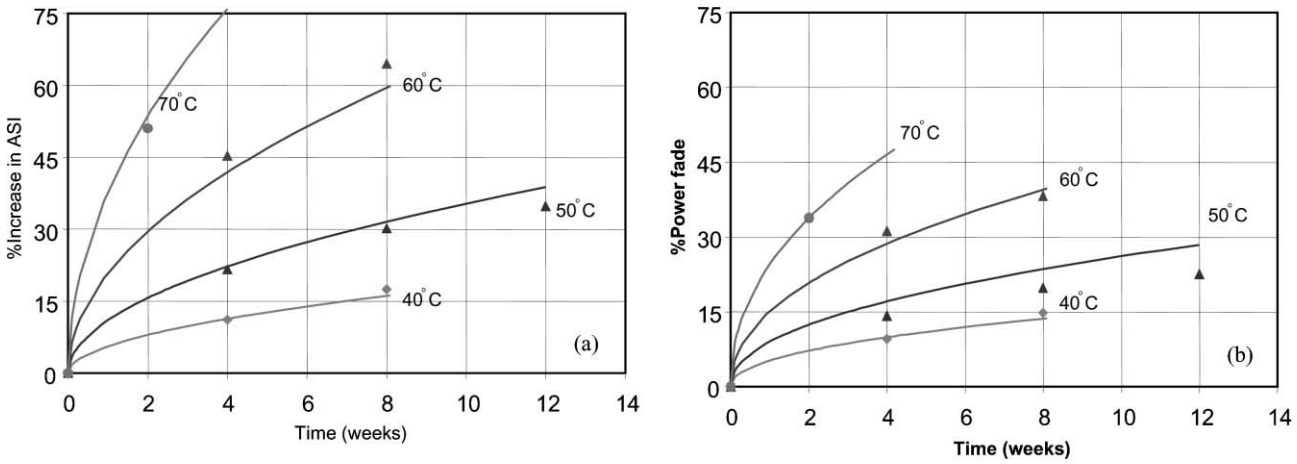

Fig. 6. (a) Increase in ASI and (b) power fade with for group A calendar life at 60% SOC. Markers represent experimental values.

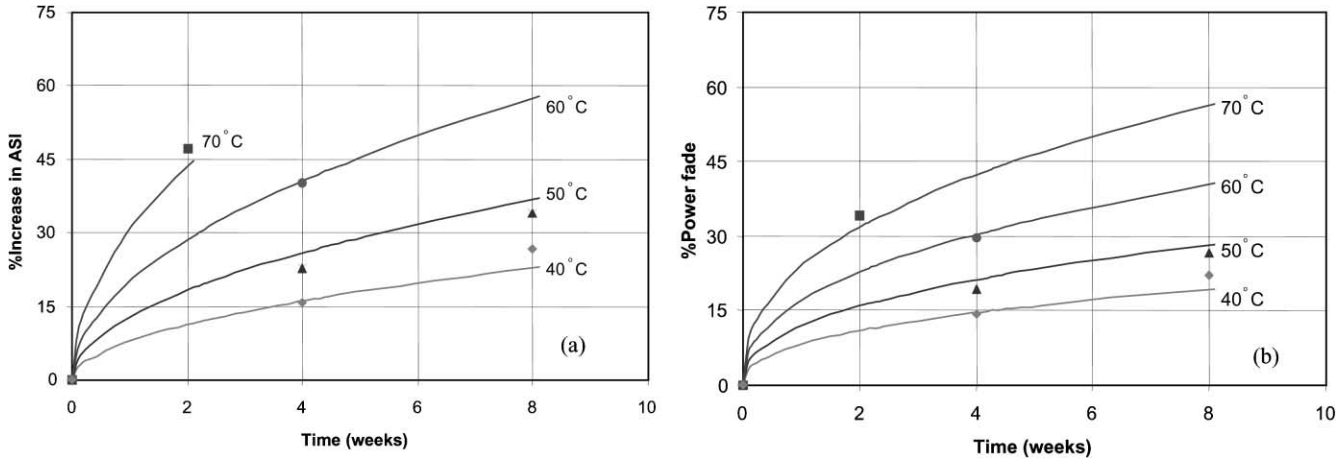

Fig. 7. Increase in ASI (a) and power fade (b) for calendar life at 60% SOC group B. Markers represent experimental values.

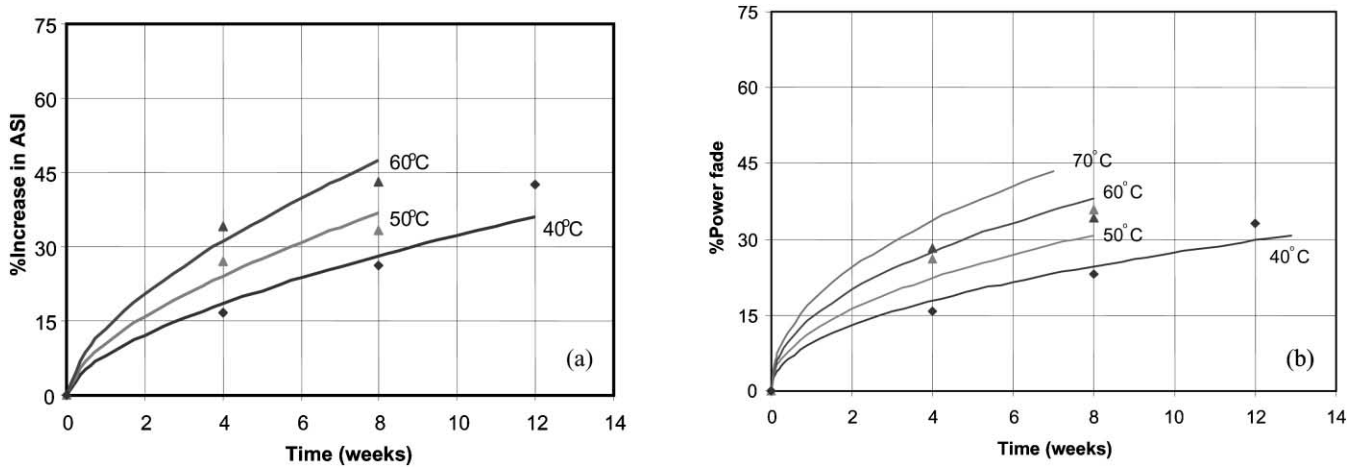

Fig. 8. Increase in ASI (a) and power fade (b) for calendar life at 80% SOC. Markers represent experimental values.

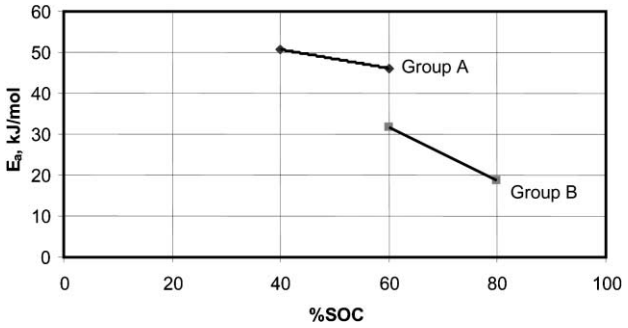

Fig. 9. An E_a vs. SOC (%) for calendar life tests.

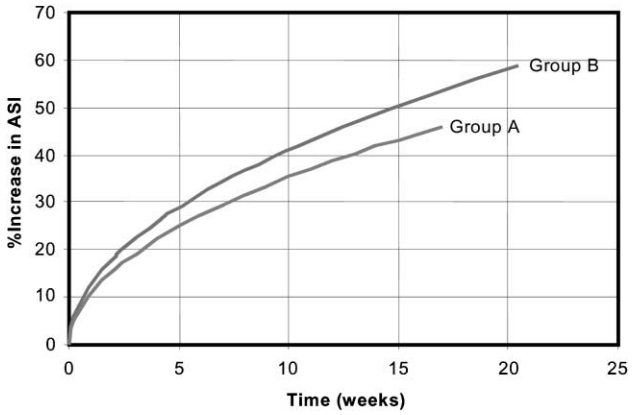

Fig. 10. Comparison of calculated values for calendar life at 50°C and 60% SOC.

the experimental values are represented by markers and the calculated values are curves.

A plot of the E_a values for the three SOCs is given in Fig. 9. In general, the trend is to lower activation energy values at higher SOCs. More importantly, there is a functionality of E_a on SOC.

The data in Table 7 suggest that the type of test used can make a difference in the results obtained. For example, using either leakage current (group A) or special calendar test (group B), the overall mechanism for ASI increase has the same dependence on time, ca. $(\text{time})^{1/2}$. However, examining the E_a/R parameters shows statistically significant differences. The activation energy for the mechanism for ASI increase is higher (56.62 ± 3.11 kJ/mol) for the leakage current test than that for the special calendar test (40.15 ± 6.32 kJ/mol).

The calculated values for groups A and B show that in the time interval studied (e.g. 50°C), there is no statistical difference between the two groups. However, since the curves for the two groups are diverging (see Fig. 10), there may be a significant difference later in cell life.

The fact that both ASI and power change with $(\text{time})^{1/2}$ implies that the data follow either 1D kinetics or some other mechanism which has $(\text{time})^{1/2}$ dependency. In the literature, the kinetics of thin-film growth have been described as having $(\text{time})^{1/2}$ dependence. Applying these concepts to the lithium-ion battery, growth of the thin-film, solid electrolyte interface (SEI) layer may be the cause of the observation [4,5]. From the data from this study, we do not know on which electrode the SEI layer is growing. However, based on literature reports [6], we think it is the SEI layer on the cathode which makes the largest contribution to the observed changes.

3.2. Cycle life

The ASI versus cell voltage and power versus cell voltage curves look very similar to those shown in Figs. 3 and 4, respectively. The changes in ASI and power versus time also follow the same general trends as those described above under calendar life. ASI increases with time and temperature, and power decreases with time and temperature.

The fitting parameters for all SOCs and ΔSOCs are given in Table 8. These fits are very good based on the values of the regression coefficient, r^2. The experimental values (markers) are given in Figs. 11–14 along with the calculated values (solid curves).

Using the data in Table 8, the values of the z parameter indicates the dependence on time and, therefore, the mechanism(s) in operation. The z for the ASI data for a given SOC is strongly dependent on the ΔSOC. At 60% SOC and 3% ΔSOC, the z value is ca. 0.50, while at 6% ΔSOC, it is ca. 0.10. In the case of power fade, at 60% SOC, there is also a marked change in mechanism going from 3 to 6%

Table 8
Fitting parameters from cycle life study

SOC (%)	ΔSOC (%)		ASI increase				Power fade			
			z	E_a/R (K)	ln A	r^2	z	E_a/R (K)	ln A	r^2
60	3	Value	0.54	3414.94	13.52	0.98	0.25	2079.32	9.49	1.00
		S.E.	0.09	368.24	1.03		0.00	1.99	0.01	
	6	Value	0.11	1881.29	9.48	0.94	0.08	1330.07	7.46	0.92
		S.E.	0.08	378.44	1.09		0.07	306.43	0.89	
80	3	Value	0.57	4648.37	17.19	0.96	0.19	2940.95	12.17	0.99
		S.E.	0.12	566.63	1.63		0.14	396.34	1.09	
	6	Value	0.15	2317.42	10.84	0.91	0.14	1739.50	8.74	0.91
		S.E.	0.10	487.42	1.40		0.07	341.04	0.98	

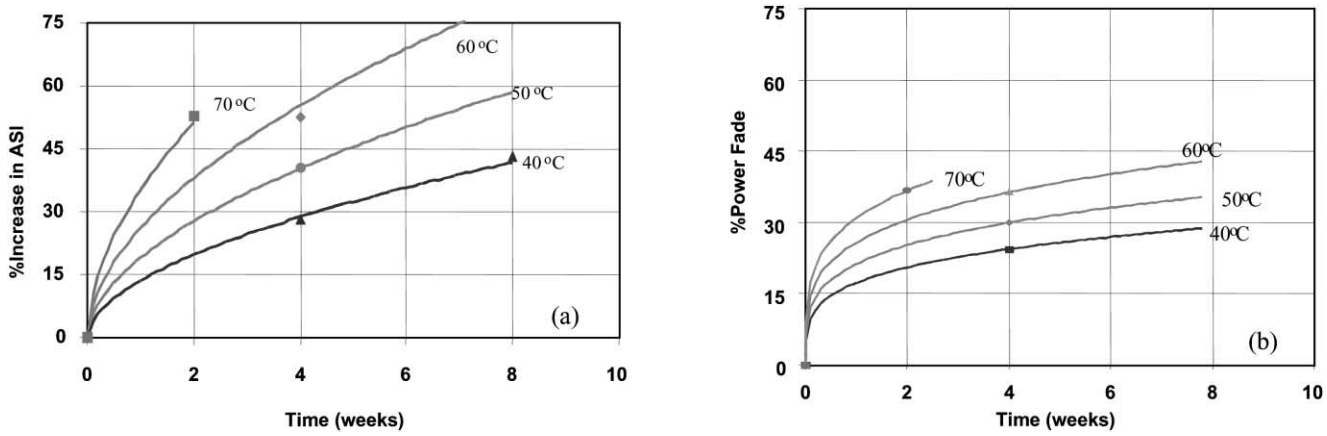

Fig. 11. (a) Increase in ASI and (b) power fade vs. time for 60% SOC, 3% ΔSOC. Markers represent experimental values.

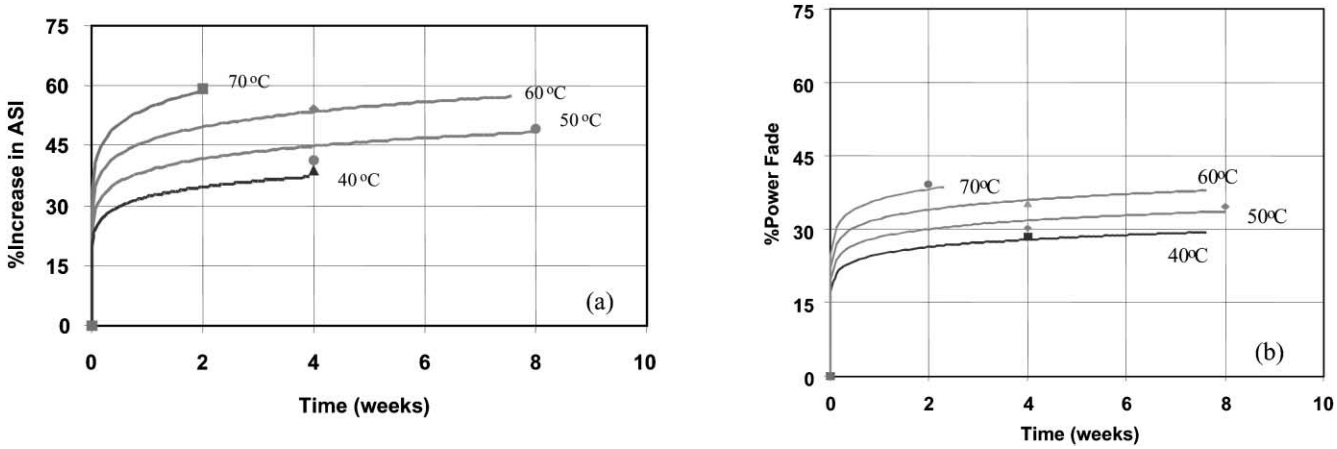

Fig. 12. (a) Increase in ASI and (b) power fade vs. time for 60% SOC, 6% ΔSOC. Markers represent experimental values.

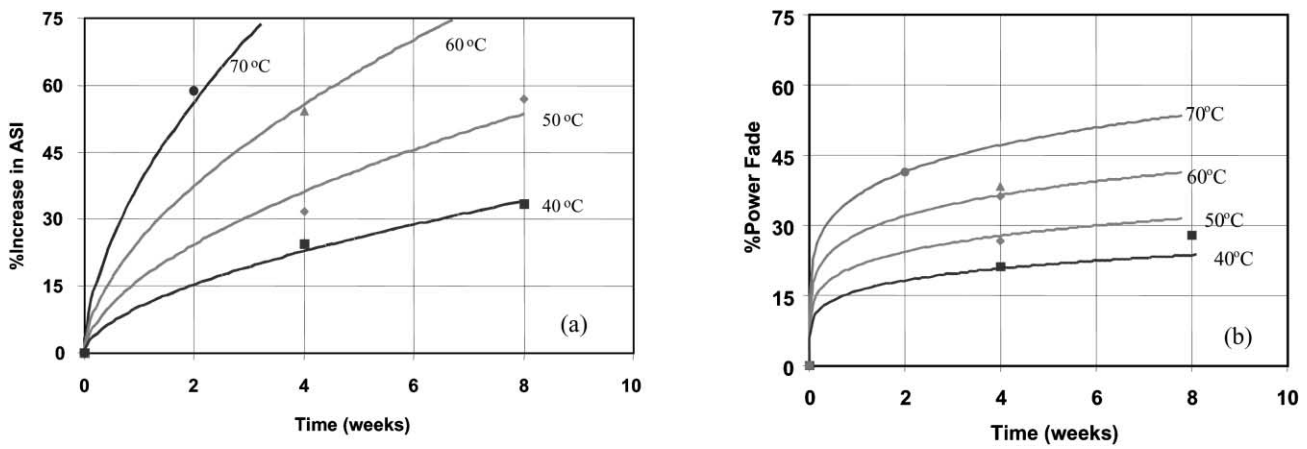

Fig. 13. (a) Increase in ASI and (b) power fade vs. time for 80% SOC, 3% ΔSOC. Markers represent experimental values.

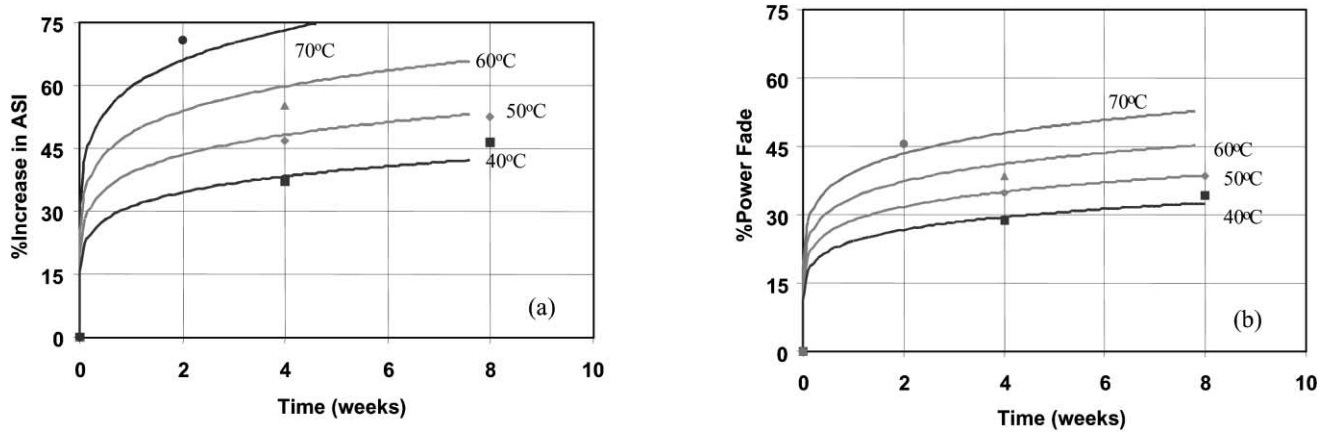

Fig. 14. (a) Increase in ASI and (b) power fade vs. time for 80% SOC, 6% ΔSOC. Markers represent experimental values.

ΔSOC, as indicated by the values of z. The situation at 80% SOC is less clear-cut. The values of z at 3% and 6% ΔSOC are not statistically different from one another, and hence, may be the same.

As discussed in the calendar life section, a z value of 1/2 indicates 1D diffusion kinetics and may be ascribed to SEI layer growth. The lower values of z indicate that a different mechanism than film growth proportional to film thickness is also causing ASI increases. Possible alternative mechanisms coming into play are the dissolution of the SEI with time, a separate reaction of the PVDF binder with the electrodes, or the reaction of $LiPF_6$ with the electrodes and/or electrolyte. A more complete discussion of the types of reactions that can occur in a Li-ion battery can be found elsewhere [7].

Adding the calculated values from 3 and 6% ΔSOC cycle life to Fig. 10 yields Fig. 15. We can clearly see that the 3% ΔSOC cycle life profile causes the ASI values to increase more rapidly than that seen in either calendar life experiment where little or no cycling occurs. However, because of a different time-dependency, the exact relationship between the 6% ΔSOC data to the results from the other experiments is not as clear.

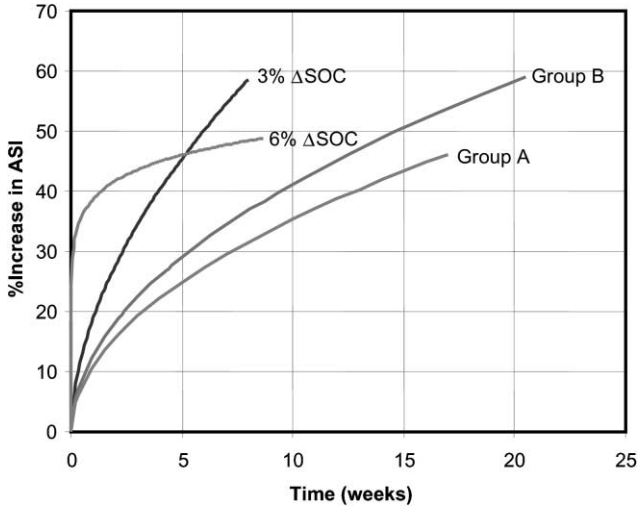

Fig. 15. Comparison of calculated values from calendar life (groups A and B), 3 and 6% ΔSOC cycle life testing.

Table 9
Calculated times to 20% power loss

Test/group	Time to 20% power fade (weeks)
40% SOC calendar life	387.21
60% SOC/A calendar life	127.64
60% SOC/B calendar life	39.37
80% SOC calendar life	11.33
60% SOC, 3% ΔSOC cycle life	6.91
60% SOC, 6% ΔSOC cycle life	0.99
80% SOC, 3% ΔSOC cycle life	38.72
80% SOC, 6% ΔSOC cycle life	1.94

Using the fitting parameters allows us to estimate the life of our Li-ion cells at 25°C. For example, if we assume that 20% power loss represents the end-of-life, the calculated times to reach this loss are given in Table 9.

From Table 9, the general trends are seen: for calendar life, cell life decreases with increasing SOC, and for cycle life, cell life decreases with ΔSOC. We did not expect to see cycle life improve with SOC (i.e. at 80% SOC). Based on the calculated values, these cells are expected to have a longer life than either cycle life population at 60% SOC. Further testing and analysis will be necessary, since this expectation was not seen in the calendar life testing. These calculated values indicate that the cell chemistry chosen does not possess a 10-year life under our test conditions.

4. Conclusions

In calendar life experiments on Li-ion cells, useful cell life was strongly affected by temperature and time. Temperature accelerated cell performance degradation. The rates of ASI increase and power fade followed simple laws based on a power of time and Arrhenius kinetics. The data have been modeled using these two concepts, and the calculated data agree well with the experimental values.

The calendar life ASI increase and power fade data follow $(\text{time})^{1/2}$ kinetics, which may be due to SEI layer growth. From the cycle life experiments, the ASI increase data follow $(\text{time})^{1/2}$ kinetics also, but there is an apparent change in overall power fade mechanism when going from 3 to 6% ΔSOC. Here, the power of time drops to a value less than 1/2, which indicates that the power fade mechanism is more complex than layer growth.

Acknowledgements

This work was performed under the auspices of the US Department of Energy, Office of Advanced Automotive Technologies, under Contract No. W-31-109-Eng-38.

References

[1] PNGV Battery Test Manual, Revision 2, August 1999, DOE/ID-10597.
[2] PNGV Battery Test Manual, Revision 2, August 1999, Appendix F.
[3] PNGV Battery Test Manual, Revision 2, August 1999, p. 32 and Fig. 2.
[4] E. Strauss, D. Golodnitsky, E. Peled, Electrochem. Solid State Lett. 2 (1999) 115–117.
[5] G. Blomgren, J. Power Sources 81-82 (1999) 112–118.
[6] K. Amine, M.J. Hammond, J. Liu, C. Chen, D.W. Dees, A.N. Jansen, G.L. Henriksen, in: Proceedings of the 10th International Meeting on Lithium Batteries, Como, Italy, 28 May–2 June 2000, p. 332.
[7] E. Peled, D. Golodnitsky, C. Menachem, D. Bar-Tow, J. Electrochem. Soc. 145 (1998) 3482–3486.